Fibre optic devices produced by arc discharges

2010 J. Opt. 12 113002

(http://iopscience.iop.org/2040-8986/12/11/113002)

IOP Publishing Journal of Optics

J. Opt. **12** (2010) 113002 (10pp) doi:10.1088/2040-8978/12/11/113002

REVIEW ARTICLE

Fibre optic devices produced by arc discharges

G Rego

Escola Superior de Tecnologia e Gestão, Instituto Politécnico de Viana do Castelo, Avenida do Atlântico, 4900-348 Viana do Castelo, Portugal
and
UOSE, INESC-Porto, Rua do Campo Alegre 687, 4169-007 Porto, Portugal

E-mail: gmrego@fc.up.pt

Received 21 June 2010, accepted for publication 20 September 2010
Published 4 November 2010
Online at stacks.iop.org/JOpt/12/113002

Abstract
We present an overview of the applications of the electric arc technique related to optical fibre technology. The use of arc discharges ranges from the well-known fibre splicing, going through the fabrication of basic devices such as fibre tapers and microspheres, to tailoring the spectra of UV-induced gratings such as in the apodization of fibre Bragg gratings and also in the fabrication of phase-shifted and sampled fibre Bragg gratings. However, in the past decade a topic more intensively investigated was probably long-period fibre gratings. Therefore, some devices based on arc-induced gratings, namely, phase-shifted and step-changed gratings and bandpass filters are discussed. We also present an electrically insulated thermocouple assembled *in situ* using arc discharges. This sensor is very useful in the determination of the temperature attained by the fibre during an arc discharge, this property being fundamental for the discussion of the mechanisms of formation and for the understanding of the thermal properties of arc-induced devices.

Keywords: long-period fibre gratings, fibre Bragg gratings, tapers, microspheres, arc discharges, temperature measurement

(Some figures in this article are in colour only in the electronic version)

1. Introduction

Among the different techniques available for the fabrication of fibre optics components, the electric arc technique is one of the few that enables their fabrication in virtually all kinds of glass fibres. This technique is simple, inexpensive and not harmful when compared to the ones based on laser radiation. Furthermore, arc-induced devices are suitable for high temperature applications since their formation mechanisms rely on thermal effects. Thus, the temperature reached by the fibre during an electric arc discharge is a key parameter to understand the properties of these devices. The main drawback of the technique is the relatively long length of the region heated by the arc (a few hundreds of micrometres) that prevents the fabrication of short-period gratings. Despite this limitation, the versatility of the technique for the fabrication of compact devices with new functionalities, such as the ones resulting from superimposing gratings on tapers or couplers or superimposing fibre Bragg gratings on arc-induced gratings, justifies a review of the applications of the electric arc technique.

As far as fibre optics technology is concerned, arc discharges were first applied to fibre fusion splicing [1, 2]. In the past thirty years this basic operation evolved due to the request for splicing dissimilar fibres which may require mode-field adjustment based on core dopant diffusion [3, 4]. On the other hand, splicing a single-mode fibre (SMF) and a photonic crystal fibre (PCF), or a SMF and a hollow optical fibre (HOF) or other combinations that may involve a multimode fibre (MMF) yields extremely useful sensors [5–8]. A core mode

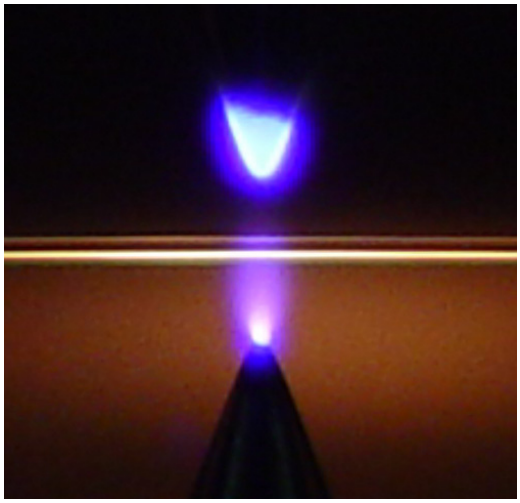

Figure 1. Photograph of the arc discharge showing its asymmetry.

blocker can also be made by concatenating a short piece of HOF in between a SMF [9].

Several other fibre optics components have been produced based on the electric arc technique. Some are just basic devices like fibre tapers [10], fibre probes [11] and microspheres [12] whilst others like fibre couplers [13] and long-period fibre gratings (LPFGs) [14] are more complex. Fibre couplers are important devices for optical communications and sensing that can be fabricated by fusion with an electric arc; two or more fibres being pulled to form a tapered structure [15–17]. The spectral response of a fibre coupler can also be modified by post-fabrication exposure to arc discharges [18, 19]. Band rejection filters have been fabricated by applying successive arc discharges in a short piece (∼3 mm) of a dispersion-shifted fibre [20].

In the past twelve years the most popular fibre optic components based on arc discharges have probably been LPFGs [21, 22] especially due to the intrinsic properties of the technique that allows the inscription in PCF fibres [23] and also to the fact that the fabricated gratings are very stable at high temperatures [24].

In this review we start by describing briefly an arc discharge and an electrically insulated thermocouple, fabricated through arc discharges, that was used to estimate the temperature reached by a fibre when exposed to an arc discharge. Some basic devices as fibre tapers, probes and microspheres are presented. Afterwards we discuss the possibility to tailor the spectra of UV-written devices by applying arc discharges, namely, the fabrication of Fabry–Perot like structures, apodization of fibre Bragg gratings (FBGs) and the inscription of sampled FBGs. Finally, we present several devices based on LPFGs, such as step-changed and phase-shift gratings, Mach–Zehnder interferometers and bandpass filters.

2. Arc discharge and fibre temperature

An arc discharge is a complex phenomenon during which a number of processes occur, namely, electrons are emitted by one electrode, due to the high intensity electric field

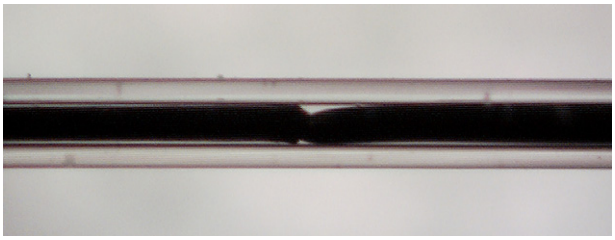

Figure 2. Photograph of an electrically insulated Pt/Pt–Rh thermocouple (wires with a diameter of 50 μm).

generated at the electrodes' tip, and while in transit between the electrodes ionize nitrogen and oxygen atoms, through impacts, creating a high temperature plasma comprising electrons and ions (figure 1) [25].

The temperature reached by a fibre when submitted to an arc discharge depends on arc parameters such as electric current and time, it depends also on the electrodes' configuration, that is, the distance between the electrodes and on the electrodes' tip (angle) and may also depend on ambient conditions. For those that have been involved in the research concerning arc-induced gratings it is unquestionable that the knowledge of this temperature is important to understand the underlying mechanisms responsible for the formation of devices based on arc discharges, such as long-period fibre gratings. In 2004, we pursued that goal through the development of a sensor that could be exposed to an arc discharge and with dimensions similar to that of an optical fibre, in order not to perturb the discharge conditions. In this context, an electrically insulated thermocouple was assembled consisting of wires of platinum and platinum/rhodium alloys placed inside a silica capillary, with internal/external diameters of 56/125 μm. The thermocouple junction (figure 2) was made by applying several arc discharges of high current. Afterwards, using the aforementioned thermocouple we estimated that the fibre reached thermal equilibrium (with a temperature of the order of 1350 °C) in less than 0.5 s, for typical arc parameters used in the fabrication of LPFGs [26, 27]. A similar temperature value was obtained by fitting to the emission spectrum of the blackbody radiation, the radiation emitted by an optical fibre during heating due to an electric arc discharge and that was detected using a Cronin spectrometer [28]. Based on this temperature value and also on the fact that for our setup the arc is directional (see figure 1), creating a temperature gradient across the fibre, the mechanisms of formation of arc-induced gratings were discussed [29, 30]. Furthermore, this electrically insulated thermocouple fabricated by applying arc discharges can find application in the calibration of the arc parameters of fusion splicing machines [31].

3. Basic devices: fibre tapers, probes and microspheres

The simplest example of a device produced by the electric arc technique is a fibre taper (figure 3(a)), which can be produced in a straightforward way by applying a time controllable arc discharge whilst the fibre is kept under a constant tension.

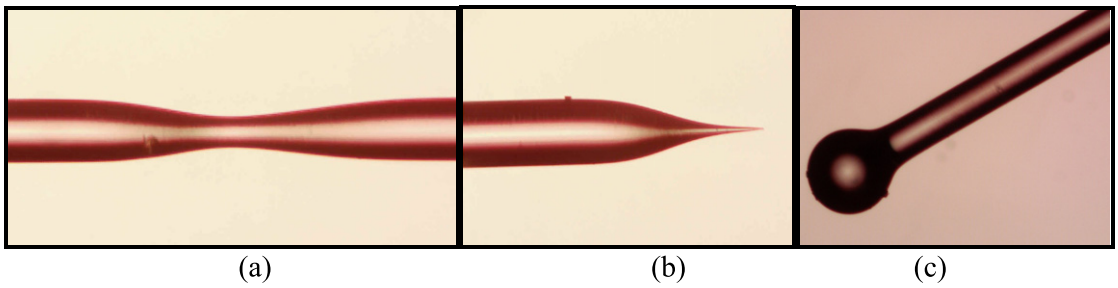

Figure 3. (a) Fibre taper. (b) Fibre probe. (c) Microsphere.

The loss evolution can be followed by an optical spectrum analyzer (or an optical power meter). The length of the taper region can be controlled by displacing the fibre during the arc discharge [10]. Tapers increase the interaction between the fibre guided modes and the surrounding medium, thus being very useful for refractive index measurement, particularly when combined with fibre gratings [32]. A severe taper can be used for laser beam shaping [33, 34]. If the previous process is further continued, a fibre probe (figure 3(b)) may be achieved, that is, the fibre is stretched until rupture, the dimensions of the fibre tip being of the order of 100 nm [11]. Optical fibre probes can be used for atomic force microscopy. Microlenses and microspheres can be produced by applying arc discharges on the tip of a fibre (figure 3(c)) [35, 36]. The former can be used for semiconductor laser–fibre coupling [35] or optical free-space interconnector [37]. The latter can act as whispering gallery mode resonators [38], side-viewing probe [39], contact-type microprobe [40] and they were also tested for blackbody radiation detection [28].

4. Tailoring the spectra of UV-written devices by using arc discharges

In this section we review the fabrication of Fabry–Perot like structures by applying arc discharges in the middle of a UV-induced FBG, the apodization of FBGs through arc discharges in the vicinity of the grating and the fabrication of sampled FBGs by writing a FBG on top of an arc-induced LPFG.

4.1. Phase-shifted Bragg gratings

Phase-shifted FBGs or Fabry–Perot like structures can be produced by applying arc discharges in the middle of a UV-induced FBG (figures 4(a) and (b)) [41, 42]. A 10 mm long Bragg grating was inscribed in a B/Ge co-doped fibre (PS 1250/1500, Fibercore) by using 248 nm laser radiation. The grating was afterwards placed under tension (caused by a weight of 5.1 g) in between the electrodes of a fusion splicing machine and was submitted to electric arc discharges of 8.5 mA and 0.5 s duration each. Figure 4(c) shows the original reflection spectrum of the grating, as well as the formation of the phase-shifted FBG after the first, second and sixth arc discharges. Figure 4(d) shows the evolution of the spectrum of the phase-shifted FBG for the third, fourth, fifth and tenth arc discharges. The arc discharges erase a short section in the middle of the FBG creating a Fabry–Perot like structure comprising two shorter gratings separated by the thermal annealed region. This is evidenced by the decrease in the peak reflectivity and by the increase in the spectral bandwidth of this structure. It is interesting to note that after five consecutive arc discharges in the same physical place the initial spectrum of the phase-shifted FBG was almost recovered, i.e., the spectra of the phase-shifted FBG correspondent to the first and sixth discharges are similar (see figure 4(c)). The same occurs for the fifth and tenth arc discharges (see figure 4(d)). The periodicity of this process resulting from a phase change of 2π remains constant even after 50 arc discharges. This behaviour may have originated from the fact that after the erasure of the short grating section, the subsequent discharges promote changes in the refractive index of the annealed region due to several mechanisms such as slight tapering and structural rearrangement in this soft fibre core [43, 44].

Recently, Cusano *et al* [45] have presented detailed analysis of these structures. They have studied the influence of the position of the arc discharges and taper waist on the interferometer spectra and, in particular, they have demonstrated, by using a simple and inexpensive technique, the feasibility of very narrow bandpass filters (FWHM = 5 pm) within the reflection band of the FBG. These devices can find application in optical communications and sensing [45–47].

4.2. Apodisation of fibre Bragg gratings

The well-known spectral response of uniform fibre Bragg gratings (FBGs) is not desirable in some optical communications applications due to the presence of side-lobes which are due to multiple reflections to and from opposite ends of the grating region [48]. The apodization of a FBG gives not only a reduction of the side-lobes but also changes its dispersion characteristics. In this section, the symmetric apodization of a FBG using electric arc discharges is presented (figure 5(a)) [49]. A uniform 5 mm long FBG centred at $\lambda_B = 1555$ nm and with a bandwidth (FWHM) of 0.3 nm was photo-imprinted, in a standard telecommunications fibre with 6 mol% GeO_2 and mode-field diameter of 10.5 ± 1.0 μm at 1550 nm (Siecor), using a diffractive phase mask illuminated with a KrF excimer laser operating at 248 nm. The fibre, placed in a motorized translation stage with a resolution of 0.1 μm, was longitudinally moved along its axis in such way that the grating was moved towards the heating zone in steps of 50 μm; 35 electric arc discharges on each side of the grating were

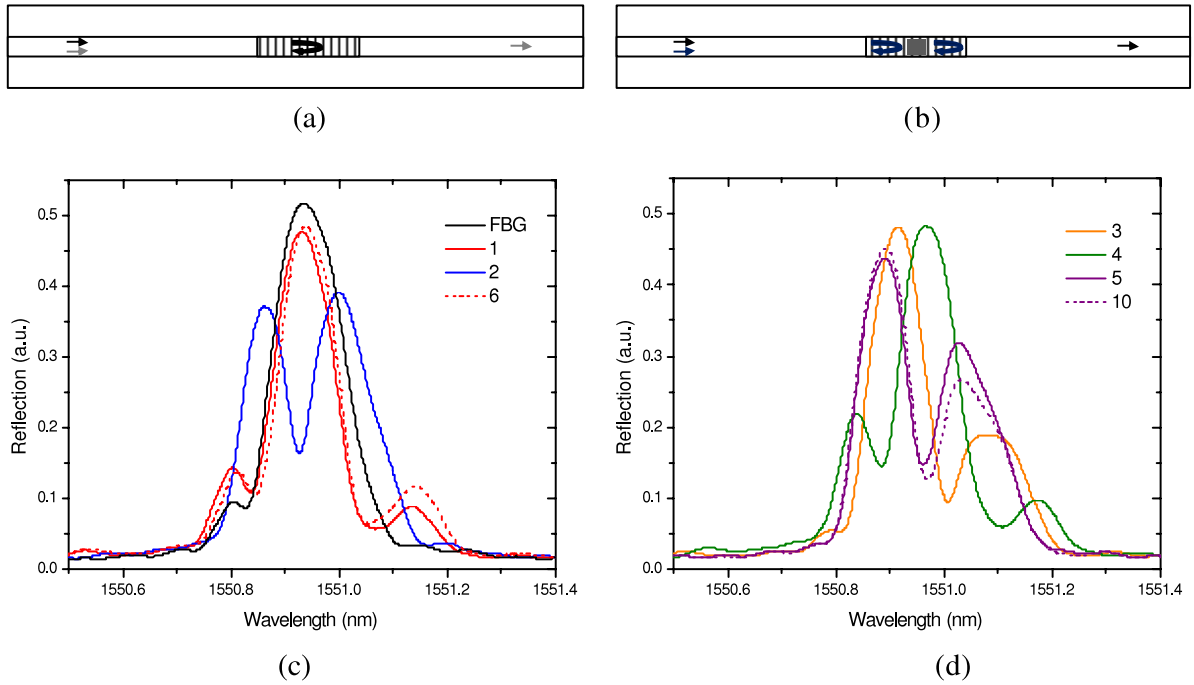

Figure 4. Schematic diagrams of (a) the FBG and (b) the phase-shifted FBG. Spectra of the phase-shifted FBG regarding the number of arc discharges: (c) 0–2 and 6; (d) 3–5 and 10.

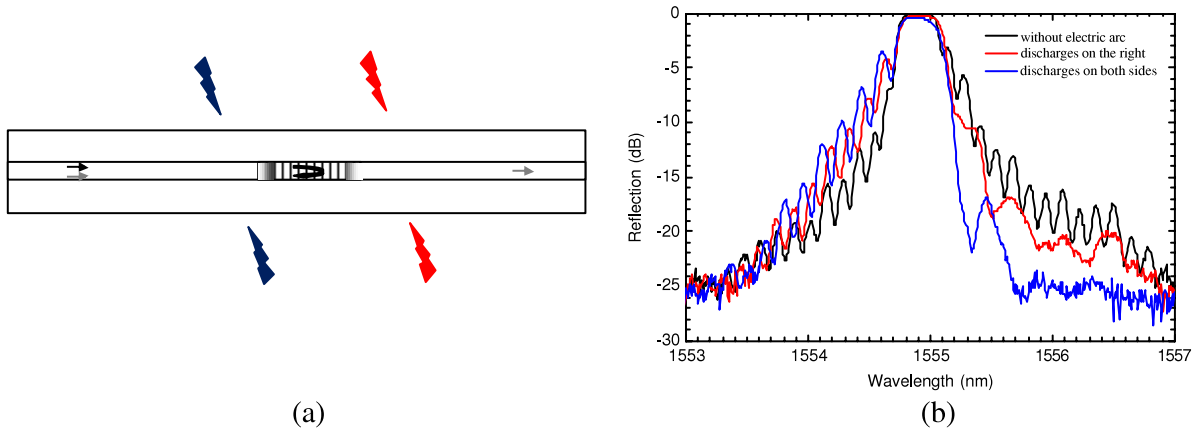

Figure 5. (a) Schematic diagram of the FBG apodization. (b) Evolution of the reflection spectrum during the apodization process. Initial FBG (solid line), FBG with 35 discharges on the right (dashed line) and FBG with 35 discharges on both sides (bold solid line).

needed to achieve the apodized grating shown in figure 5(b). The whole process was computer controlled and monitored in real time using a broadband optical source and an optical spectrum analyzer (OSA) in order to obtain the best reflection spectrum for the apodization profile.

The reflection spectrum of the grating after the apodization process (figure 5(b)) shows that the longer wavelength side-lobes were reduced due to the smoothing of the refractive index modulation profile, as caused by the high temperature annealing during the arc discharges. The pronounced structure on the short wavelength side of the grating is consistent with the formation of a distributed Fabry–Perot interferometer and corresponds to reflections at the edges of the grating (the annealed regions) [50]. The spectrum also shows a slight decrease of the peak reflectivity as expected since the refractive index modulation step profile was partially erased. These results enable one to conclude that a non-uniform effective index longitudinal distribution was obtained after the apodization process instead of the uniform FBG. Better results are expected if a preconditioning photosensitivity response and effective index profile are accomplished by exposing the fibre to the electric arc before the grating photo-inscription in the same region.

4.3. Sampled fibre Bragg gratings

A sampled fibre Bragg grating (SFBG) or superstructure grating is a contra-directional coupling grating whose effective refractive index amplitude and/or phase is modulated through a long periodic structure (figure 6(a)). The special reflection

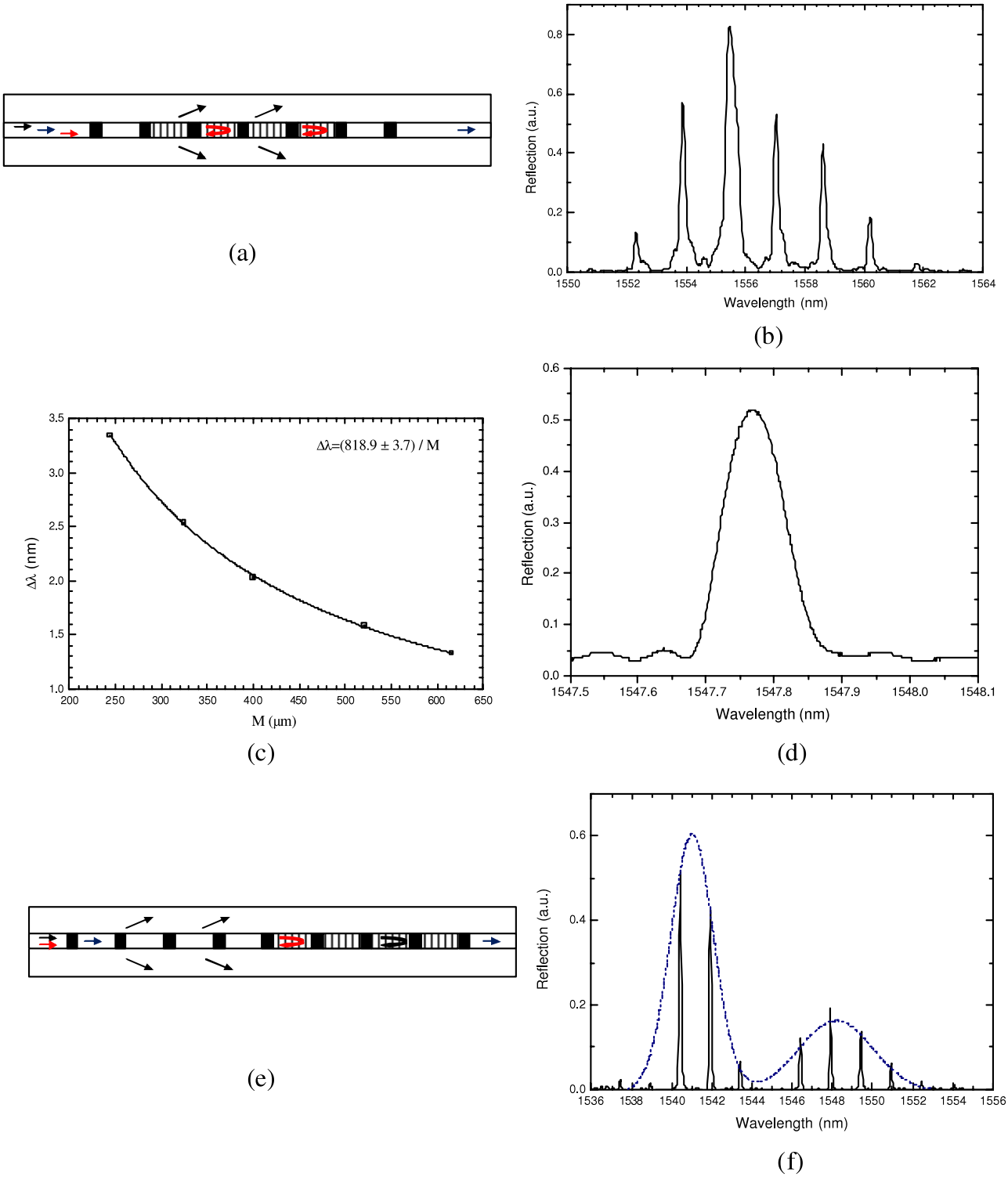

Figure 6. (a) Schematic diagram of a sampled FBG. (b) Reflection spectrum of a sampled FBG. (c) Variation of $\Delta\lambda$ with the LPFG period (M). (d) Single reflection peak from a sampled FBG. (e) Schematic diagram of a FBG written over a long LPFG in which the Bragg wavelength falls into the resonance band of the LPFG. (f) Reflection spectrum of a sampled FBG potentially originated by the core and cladding modes. The dashed lines serve as guides to the eye to delimit the two sets of reflection peaks.

characteristics of SFBGs make them very useful and attractive devices for optical communications and fibre sensors [51, 52]. The fabrication of a superstructure grating obtained by writing a FBG with a 248 nm UV source over an arc-induced LPFG comprises two different stages. In the first a LPFG (tension associated to a weight of 22.8 g, arc current smaller than 10 mA, arc duration of 1 s, modulation period of $M \sim 400\ \mu$m and grating with 66 discharges) is inscribed in a Corning dispersion-shifted fibre [14]. In the second stage a 10 mm long FBG is written over the LPFG (previously hydrogenated)

using a uniform diffractive phase mask illuminated with a KrF laser operating at 248 nm to give rise to the SFBG. The superstructure originates due to the periodic modulation of the effective refractive index amplitude caused by the reduced photosensitivity in the zones previously exposed to the electric arc (this results in a rapidly varying component with period Λ and a slowly varying envelope with a period M). The spatial frequency content of this superstructure can be approximated by a comb of delta functions centred at the Bragg frequency. In terms of reflection spectrum there will be reflection peaks separated in wavelength by $\Delta\lambda = \lambda_B^2/(2n_{\text{eff}}M)$ [53]. Separations in the range of 1.5–3.5 nm were obtained for periods M ranging from 250 to 600 μm. The reflection spectrum of a LPFG with 521 μm period and the experimentally determined variation of $\Delta\lambda$ with the period M of the LPFG are shown in figures 6(b) and (c) respectively. It can be seen that the results are in good agreement with the values derived from the theoretical equation.

An arc discharge anneals stresses, promotes structural rearrangements and may cause tapering of the fibre, all these effects contribute to changes of the effective refractive index of the fibre core. At the same time an arc discharge reduces drastically the fibre photosensitivity [54, 27]. Therefore, when a FBG is written over an arc-induced grating, only periodic regions are available for the growth of the FBG resulting in a sampled FBG. The number of reflection peaks is inversely proportional to the length of the region not annealed by the arc (the dimensions and the intensity distribution of the arc are key factors) [53]. Note, however, that FBGs have been written in tapers arc-induced in standard hydrogenated and non-hydrogenated photosensitive fibres [55, 56]. In figure 6(b) the reflected peaks seem to have an internal structure probably resulting from some 'residual' photosensitivity of the annealed regions. On the other hand, a single reflection peak belonging to another sampled FBG was swept by a wavelength tunable laser, in steps of 1 pm, the radiation being detected by an optical power meter, and no internal structure was found (see figure 6(d)). In this case, the sampled FBG was inscribed in a standard telecommunications fibre with 1.5 mol% GeO_2 and mode-field diameter of 10.5 $\pm$ 1.0 μm at 1550 nm (Sumitomo). Thus, the reduction of the fibre photosensitivity may depend not only on the arc parameters but also on the fibre composition.

Finally, when the reflection peaks fall in the same wavelength region as one LPFG resonance band it would be interesting to investigate the influence of the relative physical position between both gratings on the SFBG spectrum, that is, is it the same to write the FBG in the middle or at the edges of the LPFG? In fact, recently it was demonstrated that a FBG written 1 cm after a LPFG can partially reflect the cladding mode [57]. Therefore, it is expected that if the FBG is written at the edge of a sufficiently long LPFG a 'cladding-SFBG' may also be achieved (figure 6(e)). Although further investigations are needed, this may explain the spectrum obtained after writing a 10 mm long FBG on top of a LPFG (5.1 g, 9 mA, 1 s, 540 μm, 74 discharges) arc-induced in a B/Ge co-doped fibre (see figure 6(f)). The reflected peaks at longer wavelengths (positioned in the slope near one edge of the resonance band) may result from reflection of the core mode (similar to having the Bragg resonance outside the LPFG resonance bands) and the set of reflected peaks at shorter wavelengths (positioned near the centre of the resonance band) may result from reflection of the cladding mode.

5. Arc-induced gratings

5.1. Long-period grating based devices

A review of arc-induced gratings was presented in [22]. In the past five years other important results concerning the fabrication, characterization and sensing properties have been published in the literature. Gratings have been written in Al and Al/Er co-doped fibres [58] and also in several photonics crystal fibres [59, 60]. The fabrication of ultra-short gratings [61] and rocking filters [62] was also demonstrated. Further investigations on the thermal behaviour of arc-induced gratings at high temperatures have been presented [24, 63]. The mechanisms of formation of these gratings have also been studied intensively [29, 30, 64, 65]. As far as optical fibre sensing is concerned, these gratings, with or without thin films, can measure external refractive index changes [66–69], pressure [70] and bending [71], operate as an inclinometer [72], and simultaneously measure temperature and strain [73], while also being able to operate in harsh environments [74]. Temperature compensated sensors can be implemented by using a dual resonance formed by different mechanisms in B/Ge co-doped fibres [75]. LPFGs find a huge number of applications in optical communications and sensing fields such as gain flattening, external refractive index detection and the simultaneous measurement of temperature and strain [76–78, 73].

A LPFG is a periodic structure inscribed in the fibre that couples light between the core mode and co-propagating cladding modes at specific resonance wavelengths (figure 7(a)) [79]. The grating behaves as a selective filter where the resonance wavelengths depend on physical parameters, such as temperature and strain. The grating's spectrum can be modified by changing the fabrication parameters (arc duration, electric current and pulling tension) leading, for instance, to a step-changed grating (see figure 7(b)) where the resonances exhibit different sensitivities to changes of physical parameters and are thus very useful for multiparameter sensing [73]. Figure 7(c) shows the spectra of a typical grating and a step-changed grating (a duplication of each resonance is observed) where the electric current and pulling tension were changed after the fifteenth discharge.

The typical loss band of a LPFG can be converted into a bandpass by inserting a phase shift in the middle of the grating during its fabrication. This can be accomplished by applying one or more arc discharges in the middle of a LPFG (figure 8(a)). Figure 8(b) shows a π-shift grating obtained after submitting a LPFG, induced in the aforementioned Sumitomo fibre, to five extra arc discharges applied to its centre. Alternatively, a phase shift in the middle of the grating is produced by changing the grating pitch by half a period (figure 8(c)) [80]. Figure 8(d) shows the initial

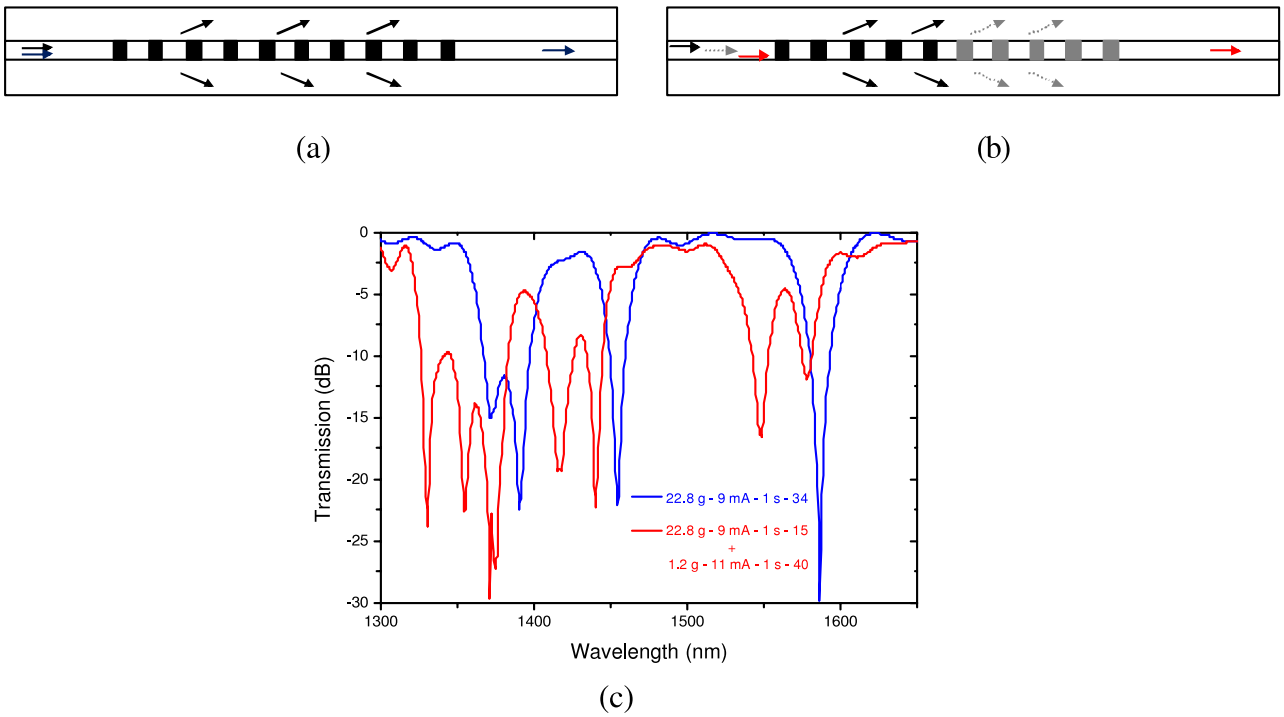

Figure 7. Schematic diagram of (a) a LPFG and (b) a step-changed LPFG. (c) Spectrum of a typical grating and of a step-changed grating.

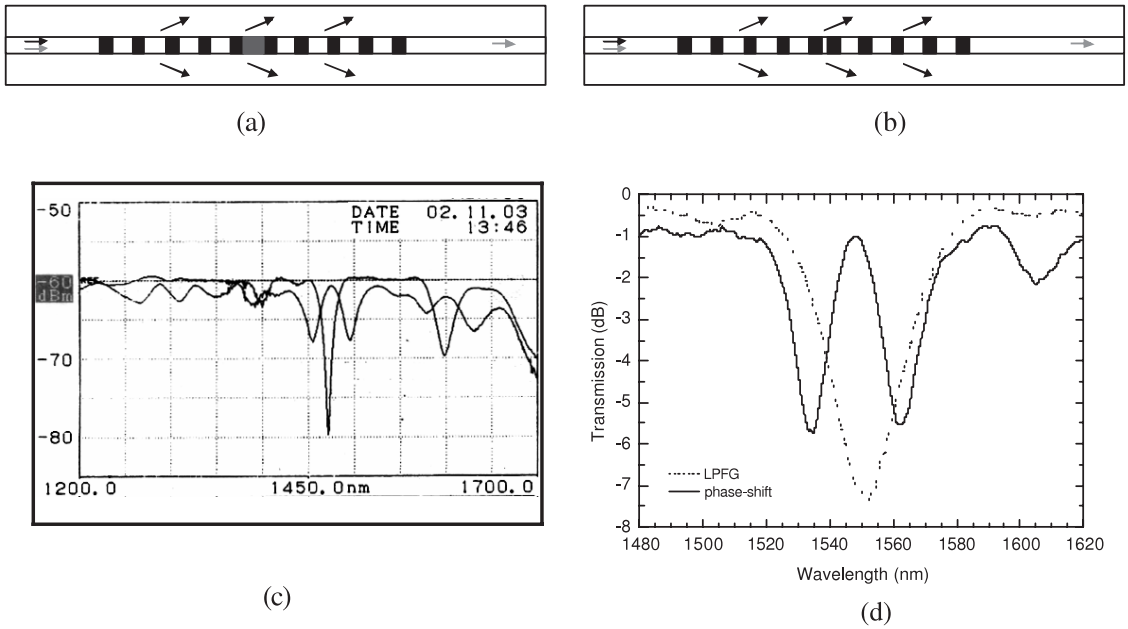

Figure 8. (a) Schematic diagram of a phase-shifted LPFG by Δn modulation; (b) π-shift produced after five arc discharges in the middle of the grating; (c) schematic diagram of a phase-shifted LPFG by introducing a gap between two consecutive grating sections; (d) grating transmission spectra before and after the phase shift.

and final spectra of a phase-shift grating arc-induced in standard telecommunications fibre (SMF-28, Corning) using the following fabrication parameters: weight of 5.1 g, a period of 540 μm, an electric current of 9.5 mA, an arc duration of 1 s, and 35 discharges were produced on each side of the phase-shift region (displacement of 118 μm) [81].

The concatenation of two identical LPFGs leads to the well-known Mach–Zehnder interferometer (figure 9(a)). One half of the light is coupled from the fundamental mode to the cladding mode and the other half goes through the core. These two paths can be seen as arms of an interferometer, since the light that is guided by the cladding is coupled back by the second grating and interferes with the light guided by the core. Figure 9(b) shows the transmission spectrum of two LPFGs arc-induced in the B/Ge co-doped fibre (5.1 g, 9 mA, 0.5 s, 425 μm, 60 discharges), each having a transmission loss of

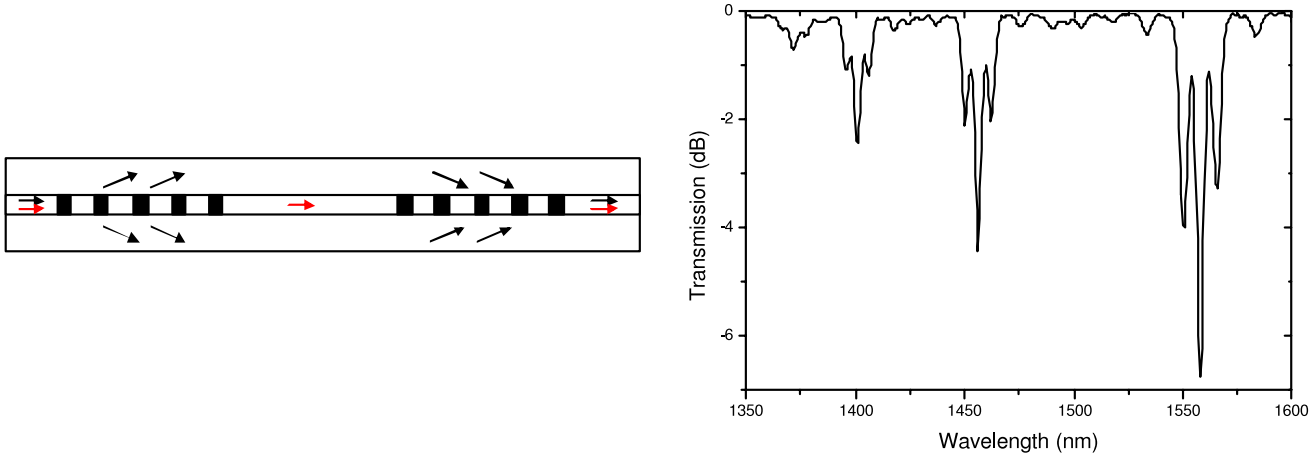

Figure 9. (a) Schematic diagram of a Mach–Zehnder interferometer based on LPFGs; (b) transmission spectrum of two concatenated LPFGs separated by ∼25 mm.

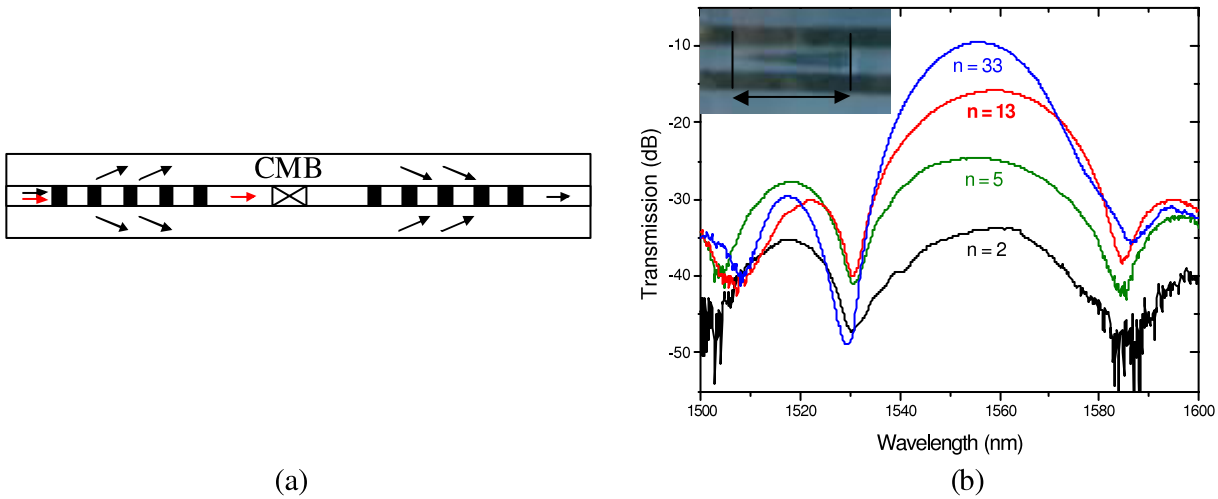

Figure 10. (a) Schematic diagram showing the effect of a core mode blocker in between two LPFGs. (b) Evolution of the transmission spectrum of the bandpass filter for different numbers of turns. Inset: typical photograph of the region containing the tapered capillary after splicing.

3 dB at 1.55 μm. If a taper is fabricated in the region between the gratings an interferometer highly sensitive to variations of the external refractive index is achieved [82, 32]. Recently, another interesting interferometer comprising a LPFG and an arc-induced point defect in a photonic crystal fibre was proposed by Choi *et al* [83].

5.2. Core mode blockers

A core mode blocker (CMB) is an obstacle inserted in the fibre core that prevents the propagation of light in the core, being the key element for the fabrication of bandpass filters based on LPFGs (see figure 10(a)) [84]. Typically, the CMB is achieved by exposing the fibre to a high temperature heat source, such as intense laser radiation [84–86] or arc discharges [87]. The latter was demonstrated by exposure of a hydrogenated B/Ge co-doped fibre to arc discharges that led to a micro-explosion in the core. Thus, the core of the fibre is destroyed such that light is no longer guided by the fundamental mode. When a CMB is inserted in between two identical concatenated LPFGs, the light that is rejected by the first grating is afterwards coupled back by the second one, the transmission spectrum of the bandpass filter being similar to the inverted spectrum of the individual gratings. Note, however, that since a fraction of the energy of a cladding mode is guided by the fibre core, the CMB leads to bandpass filters with typical insertion loss values of 1–2 dB [84–87].

A different approach to having the fundamental mode blocked and that can be applied to any kind of fibre is splicing a short section (0.3–0.5 mm) of a silica capillary in between a single-mode fibre. The inset of figure 10(b) shows a photograph of a CMB fabricated by that technique. However, due to the dimensions of the capillary (inside diameter: 25 μm) used, several arc discharges were applied in the splice region in order to reduce its diameter. It was experimentally determined that tapering the capillary, from the side of the incoming

light, would lead to bandpass filters with lower insertion loss. The performance of the CMB as an element of a bandpass filter was evaluated in the laboratory, in a straightforward way, by using mechanically induced long-period fibre gratings (MLPFGs) [88].

Two MLPFGs were fabricated by winding a nylon string around the fibre/grooved tube set on both sides of the CMB section. The evolution of the transmission spectrum of the bandpass filter as a function of the number of turns of the nylon string is shown in figure 10(b). The lowest insertion loss (10 dB) and the highest non-resonant light suppression (20 dB) were obtained after 33 turns, however the side-lobes in the transmission spectrum are asymmetric. The high insertion loss results from the large diameter of the capillary used being much larger than the fibre core diameter. By using a capillary with an inside diameter of 6 μm the insertion loss can be reduced to 3–4 dB [9]. The non-resonant light suppression is typically about 20 dB, although the technique based on the micro-explosion may achieve larger values [87]. The bandwidth (FWHM) was 18.6 nm which is three times larger than that obtained in [87] and one order of magnitude larger than that obtained in [84] and [86].

Recently, a technique based on femtosecond laser ablation of the core was demonstrated that can also be applied to any kind of fibre [89]. The obtained results are comparable to the ones achieved by other techniques relying on damage due to laser radiation. Bandpass filters are very important in the optics communication field and several applications have been proposed in the literature [90, 91].

6. Conclusions

We have reviewed the potentialities of the electric arc technique to produce optical fibre devices. In particular, we presented the fabrication of Fabry–Perot like structures, the apodization of fibre Bragg gratings and the inscription of sampled FBGs. Fibre components based on arc-induced LPFGs were also discussed, namely, phase-shifted and step-changed gratings.

Acknowledgments

The author would like to thank J L Santos, F Faramarz, O V Ivanov, P V S Marques, L A Ferreira and F M Araújo for their valuable comments. The author also thanks P Caldas for supplying the photos shown in figure 1 and R Romero for supplying material concerning sampled fibre Bragg gratings.

References

[1] Bisbee D L 1976 *Appl. Opt.* **15** 796–8
[2] Hatakeyama I and Tsuchiya H 1978 *Appl. Opt.* **17** 1959–64
[3] Shiraishi K, Aizawa Y and Kawakami S 1990 *J. Lightwave Technol.* **8** 1151–61
[4] Dianov E M, Karpov V I, Grekov M V, Golant K M, Vasiliev S A, Medvedkov O I and Khrapko R R 1997 *Proc. 11th Int. Conf. on Integrated Optics and Optical Fibre Communications* vol 2, pp 53–6
[5] Villatoro J, Finazzi V, Coviello G and Pruneri V 2009 *Opt. Lett.* **34** 2441–3
[6] Coviello G, Finazzi V, Villatoro J and Pruneri V 2009 *Opt. Express* **17** 21551–9
[7] Choi H Y, Mudhana G, Park K S, Paek U-C and Lee B H 2010 *Opt. Express* **18** 141–9
[8] Wang X, Xu J, Zhu Y, Cooper K L and Wang A 2006 *Opt. Lett.* **31** 885–7
[9] Choi S, Eom T J, Yu J W, Lee B H and Oh K 2002 *IEEE Photon. Technol. Lett.* **14** 1701–3
[10] Ishikura A, Kato Y and Miyauchi M 1986 *Appl. Opt.* **25** 3460–5
[11] Lin H N, Lewlomphaisarl U, Chen S H, Lee L J and Tsai D P 1998 *Rev. Sci. Instrum.* **69** 3843–5
[12] Fan K-C, Hsu H-Y, Hung P-Y and Wang W 2006 *J. Opt. A: Pure Appl. Opt.* **8** 782–7
[13] Chiang K S 2009 *Appl. Opt.* **48** F61–7
[14] Rego G, Okhotnikov O, Dianov E and Sulimov V 2001 *J. Lightwave Technol.* **19** 1574–9
[15] Wang B and Mies E 2009 *Proc. SPIE* **6781** 678130
[16] Belovolov M I, Guryanov A N, Gusovski D D, Dianov E M, Dyankov G L and Kuznetsov A V 1985 *Sov. J. Quantum Electron.* **15** 1238–42
[17] Araújo F M 1999 *PhD Thesis* University of Porto
[18] Morishita K and Ohta N 2008 *J. Lightwave Technol.* **26** 1915–20
[19] Karpov V I, Grekov M V, Dianov E M, Golant K M, Vasiliev S A, Medvedkov O I and Khrapko R R 1998 *Proc. Optical Fiber Commun.* **2** 279–80 (Optical Society of America)
[20] Mata-Chávez R I, Martinez-Rios A, Torres-Gomez I, Alvarez-Chavez J A, Selvas-Aguilar R and Estudillo-Ayala J 2008 *Opt. Laser Technol.* **40** 671–5
[21] Kosinski G and Vengsarkar A M 1998 *Proc. Optical Fiber Communications* vol 2, pp 278–9 (Optical Society of America) ThG3
[22] Rego G, Marques P S, Salgado H M and Santos J L 2005 *Fiber Integr. Opt.* **24** 245–9
[23] Humbert G, Malki A, Fevrier S, Roy P and Pagnoux D 2003 *Electron. Lett.* **39** 349–50
[24] Rego G 2009 *Electron. Lett.* **45** 972–4
[25] Cobine J D 1941 *Gaseous Conductors* (New York: Mc-Graw Hill)
[26] Rego G, Santos L M B N F, Schröder B, Marques P V S, Santos J L and Salgado H M 2004 *IEEE Photon. Technol. Lett.* **16** 2111–4
[27] Rego G, Santos L M B N F and Schröder B 2008 *Microwave Opt. Technol. Lett.* **50** 2020–5
[28] Rego G, Marques P V S, Santos J L and Salgado H M 2006 *Opt. Commun.* **259** 620–5
[29] Rego G, Ivanov O and Marques P V S 2006 *Opt. Express* **14** 9594–9
[30] Ivanov O and Rego G 2007 *Opt. Express* **15** 13936–41
[31] Rego G, Marques P V S, Santos L M N B F, Schröder B, Santos J L and Salgado H M 2006 *Portuguese Patent* 103160
[32] Caldas P, Jorge P A S, Araújo F, Ferreira L A, Rego G and Santos J L 2009 *Proc. SPIE* **7503** 750349
[33] Tian Z, Nix M and Yam S-H 2009 *Opt. Lett.* **34** 229–31
[34] Alvarez-Chavez J A, Grudinin A B, Nilsson J, Turner P W and Clarkson W A 1999 *Proc. Conf. on Lasers and Electro-Optics* CWE7
[35] Kuwahara H, Sasaki M and Tokoyo N 1980 *Appl. Opt.* **19** 2578–83
[36] Caldas P *et al* 2010 *Proc. SPIE* **7653** 76532P
[37] Kong G-J, Kim J, Choi H-Y, Im J E, Park B-H, Paek U-C and Lee B H 2006 *Opt. Lett.* **31** 894–6
[38] Zervas M N, Murugan G S and Wilkinson J S 2008 *Proc. Int. Conf. on Transparent Optical Networks* vol 4, pp 58–60

[39] Choi H Y, Ryu S Y, Na J, Lee B H, Sohn I-B, Noh Y-C and Lee J 2008 *Opt. Lett.* **33** 34–6
[40] Fan K-C, Wang W and Hsu H-Y 2008 *J. Micromech. Microeng.* **18** 015011
[41] Uttanchandani D and Othonos A 1996 *Opt. Commun.* **127** 200–4
[42] Rego G, Santos J L and Salgado H M 2003 *Proc. I Symp. on Enabling Optical Networks* pp 5–6
[43] Rego G and Ivanov O 2007 *Opt. Lett.* **32** 2984–6
[44] Grubsky V and Feinberg J 2005 *Opt. Lett.* **30** 1279–81
[45] Cusano A, Iadicicco A, Paladino D, Campopiano S and Cutolo A 2008 *Opt. Express* **16** 15332–42
[46] Paladino D, Iadicicco A, Campopiano S and Cusano A 2009 *Opt. Express* **17** 1042–54
[47] Frazão O, Silva S F O, Guerreiro A, Santos J L, Ferreira L A and Araújo F M 2008 *Appl. Opt.* **46** 8578–82
[48] Othonos A 1997 *Rev. Sci. Instrum.* **68** 4329–41
[49] Romero R, Rego G and Marques P V S 2008 *Microwave Opt. Technol. Lett.* **50** 316–9
[50] Mizahri V and Sipe J E 1993 *J. Lightwave Technol.* **11** 1513–7
[51] Frazão O, Romero R, Rego G, Marques P V S, Salgado H M and Santos J L 2002 *Electron. Lett.* **38** 693–5
[52] Romero R, Frazão O, Rego G, Marques P V S and Salgado H M 2002 *Proc. Course on Photosensitivity in Optical Waveguides and Glasses* 43/WA5
[53] Romero R 2004 *PhD Thesis* University of Porto
[54] Malo B, Albert J, Johnson D C, Bilodeau F and Hill K O 1992 *Electron. Lett.* **28** 1598–9
[55] Frazão O, Melo M, Marques P V S and Santos J L 2005 *Meas. Sci. Technol.* **16** 984–8
[56] Byron K C, Sugden K, Bricheno T and Bennion I 1993 *Electron. Lett.* **29** 1659–60
[57] Han M, Guo F and Lu Y 2010 *Opt. Lett.* **35** 399–01
[58] Rego G, Falate R, Fabris J L, Santos J L, Salgado H M, Semjonov S L and Dianov E M 2005 *Opt. Lett.* **30** 2065–7
[59] Iredale T B, Steinvurzel P and Eggleton B J 2006 *Electron. Lett.* **42** 739–40
[60] Petrovic J S, Dobb H, Mezentsev V K, Kalli K, Webb D J and Bennion I 2007 *J. Lightwave Technol.* **25** 1306–12
[61] Nam S H, Zhan C, Lee J, Hahn C, Reichard K, Ruffin P, Deng K L and Yin S Z 2005 *Opt. Express* **13** 731–7
[62] Statkiewicz-Barabach G, Anuszkiewicz A, Urbanczyk W and Wojcik J 2008 *Opt. Express* **16** 17258–68
[63] Morishita K and Kaino A 2005 *Appl. Opt.* **44** 5018–23
[64] Durr F, Rego G, Marques P V S, Semjonov S L, Dianov E, Limberger H G and Salathé R P 2005 *J. Lightwave Technol.* **23** 3947–53
[65] Rego G, Dürr F, Marques P V S and Limberger H G 2006 *Electron. Lett.* **42** 334–5
[66] Pilla P, Foglia Manzillo P, Giordano M, Korwin-Pawlowski M L, Bock W J and Cusano A 2008 *Opt. Express* **16** 9765–80
[67] Smietana M, Korwin-Pawlowski M L, Bock W J, Pickrell G R and Szmidt J 2008 *Meas. Sci. Technol.* **19** 085301
[68] Falate R, Kamikawachi R C, Muller M, Kalinowski H J and Fabris J L 2005 *Sensors Actuators* B **105** 430–6
[69] Possetti G R C, Kamikawachi R C, Prevedello C L, Muller M and Fabris J L 2009 *Meas. Sci. Technol.* **20** 034003
[70] Bock W J, Chen J, Mikulic P and Eftimov T 2007 *IEEE Trans. Instrum. Meas.* **56** 1176–80
[71] Frazão O, Falate R, Baptista J M, Fabris J L and Santos J L 2005 *Opt. Eng.* **44** 110502
[72] Frazão O, Falate R, Fabris J L, Santos J L, Ferreira L A and Araújo F M 2006 *Opt. Lett.* **31** 2960–2
[73] Rego G, Falate R, Ivanov O and Santos J L 2007 *Appl. Opt.* **46** 1392–6
[74] Rego G, Fernandez Fernandez A, Gusarov A, Brichard B, Berghmans F, Santos J L and Salgado H M 2005 *Appl. Opt.* **44** 6258–63
[75] Caldas P, Rego G, Ivanov O and Santos J L 2010 *Appl. Opt.* **49** 2994–9
[76] Slavík R and Kulishov M 2007 *Opt. Lett.* **32** 757–9
[77] Chen X, Zhang L, Zhou K, Davies E, Sugden K, Bennion I, Hughes M and Hine A 2007 *Opt. Lett.* **32** 2541–3
[78] Pilla P, Giordano M, Korwin-Pawlowski M L, Bock W J and Cusano A 2007 *IEEE Photon. Technol. Lett.* **19** 1517–9
[79] Vengsarkar A, Lemaire P, Judkins J, Bhatia V, Erdogan T and Sipe J 1996 *J. Lightwave Technol.* **14** 58–65
[80] Humbert G and Malki A 2003 *Electron. Lett.* **39** 1506–7
[81] Falate R, Frazao O, Rego G, Fabris J L and Santos J L 2006 *Appl. Opt.* **45** 5066–72
[82] Ding J F, Zhang A P, Shao L Y, Yan J H and He S L 2005 *IEEE Photon. Technol. Lett.* **17** 1247–9
[83] Choi H Y, Park K S and Lee B H 2008 *Opt. Lett.* **33** 812–4
[84] Starodubov D S, Grubsky V and Feinberg J 1998 *IEEE Photon. Technol. Lett.* **10** 1590–2
[85] Dimmick T, Satorius D A and Burdge G L 2001 *Proc. Optical Fiber Communication Conf. (Optical Society of America)* WJ3
[86] Lee K J, Yeom D I and Kim B Y 2007 *Opt. Express* **15** 2987–92
[87] Han Y G, Kim S H, Lee S B, Paek U-C and Chung Y 2003 *Electron. Lett.* **39** 1107–8
[88] Rego G, Fernandes J R A, Santos J L, Salgado H M and Marques P V S 2003 *Opt. Commun.* **220** 111–8
[89] Lim S D, Kim J G, Lee K, Lee S B and Kim B Y 2009 *Opt. Express* **17** 18449–54
[90] Choi S, Oh K, Shin W, Park C S, Paek U-C, Park K J, Chung Y C, Kim G Y and Lee Y G 2002 *IEEE Photon. Technol. Lett.* **14** 248–50
[91] Han Y, Kim S and Lee S 2004 *Opt. Express* **12** 1902–7